Heliyon 6 (2020) e05357

Contents lists available at ScienceDirect

Heliyon

journal homepage: www.cell.com/heliyon

Research article

PXR is a target of (-)-epicatechin in skeletal muscle

Miguel Ortiz-Flores [a], Andrés Portilla-Martínez [a], Francisco Cabrera-Pérez [a], Nayelli Nájera [a], Eduardo Meaney [a], Francisco Villarreal [b], Javier Pérez-Durán [c], Guillermo Ceballos [a,*]

[a] Escuela Superior de Medicina, Instituto Politécnico Nacional, Salvador Díaz Mirón esq. Plan de San Luis S/N, Miguel Hidalgo, Casco de Santo Tomas, 11340 Ciudad de México, CDMX, Mexico
[b] Medical School, University of California San Diego, 9500 Gilman Dr, La Jolla, CA 92093, USA
[c] Instituto Nacional de Perinatología, Calle Montes Urales 800, Lomas - Virreyes, Lomas de Chapultepec IV Secc, 11000 Ciudad de México, CDMX, Mexico

ARTICLE INFO

Keywords:
Bioinformatics
Theoretical computer science
Cell biology
Proteins
Biochemistry
Molecular biology
(-)-Epicatechin
Mannich type reaction
Affinity column
PXR
Cyp3a11
Differentiation

ABSTRACT

(-)-Epicatechin (EC) is a flavanol that has shown numerous biological effects such as: decrease risk of cardiovascular dysfunction, metabolism regulation, skeletal muscle (SkM) performance improvement and SkM cells differentiation induction, among others. The described EC acceptor/receptor molecules do not explain the EC's effect on SkM. We hypothesize that the pregnane X receptor (PXR) can fulfill those characteristics, based on structural similitude between EC and steroidal backbone and that PXR activation leads to similar effects as those induced by EC. In order to demonstrate our hypothesis, we: 1) analyzed the possible EC and mouse PXR interaction through in silico strategies, 2) developed an EC's affinity column to isolate PXR, 3) evaluated, in mouse myoblast (C2C12 cells) the inhibition of EC-induced PXR's nucleus translocation by ketoconazole, a specific blocker of PXR and 4) analyzed the effect of EC as an activator of mouse PXR, evaluating the expression modulation of cytochrome 3a11 (Cyp3a11) gen and myogenin protein. (-)-Epicatechin interacts and activates PXR, promoting this protein translocation to the nucleus, increasing the expression of Cyp3a11, and promoting C2C12 cell differentiation through increasing myogenin expression. These results can be the base of further studies to analyze the possible participation of PXR in the skeletal muscle effects shown by EC.

1. Introduction

Catechins are a family of secondary metabolites found in a wide diversity of vegetal products; this family of flavonoids includes (-)-Epicatechin (EC), (-)-Epicatechin gallate (ECG) and (-)-Epigallate catechin gallate (EGCG). Among them, (-)-Epicatechin is found mainly in cacao beans, which have the highest content of total flavanols (120–180 g/kg), of which 35% correspond to EC [1].

This flavanol has shown numerous biological effects such as: decrease risk of cardiovascular dysfunction, metabolism regulation, skeletal muscle cells differentiation induction, among others [2, 3, 4, 5, 6, 7]. However, despite its various positive effects there is little evidence demonstrating the mechanism(s) through which EC initiates those effects.

It has been proposed that EC improves cardiovascular dysfunction trough the activation of plasmalemma-associated G protein-coupled estrogen receptor (GPER) which mediate, at least partially, the effects of this flavonoid in endothelial cells in culture, showing a similar response to the synthetic GPER's specific agonist (G1), and also partially blocked by a selective antagonist (G15), suggesting an agonist-acceptor/receptor type interaction [8].

Nevertheless, the effects of EC through this type of proteins seem not to be universal since in SkM the effects of EC, such as the increased expression of proteins that in turn induced mitochondrial biogenesis, muscular growth and differentiation regulation [4, 9], are not at all mediated by GPER.

In order to identify proteins that could mediate the EC's skeletal muscle effects and based on: 1) results showing that EC effects are specific/selective [10], 2) specificity seems to depend on EC molecular chiral centers and 3) EC's structural similitude with steroidal backbone, we analyzed proteins with receptor characteristics that can recognize steroids and whose activation/deactivation leads to similar effects to those observed for EC.

Pregnane X receptor (PXR) is one of the possible acceptor/effector proteins; although its main function is xenobiotics depuration, it is also linked to metabolism regulation and cell proliferation [11, 12, 13, 14, 15,

* Corresponding author.
E-mail address: gceballosr@ipn.mx (G. Ceballos).

https://doi.org/10.1016/j.heliyon.2020.e05357
Received 19 June 2020; Received in revised form 21 September 2020; Accepted 23 October 2020

16, 17, 18, 19, 20, 21]. In order explore the possible EC-PXR interaction, we used several experimental approaches: 1) analyzed the possible interaction through affinity score, via molecular docking. 2) developed an affinity column, immobilizing an EC's Mannich derivative to an agarose matrix, leading the flavonoid chiral centers free, preserving its stereochemical characteristics and 3) evaluated the EC-induced PXR activation in cultured C2C12 myoblast cells, analyzing the receptor's translocation, the effect on the expression of Cyp3a11 [22], a well characterized downstream gen activated after the binding of specific ligand(s) to PXR, and its possible participation on C2C12 differentiation.

On this regard, some attempts had been implemented to search proteins that can interact with EC as example: exchange columns to determine structural identifiers of EC and (+)-catechin required for their interaction with an specific flavonoid enzyme in vegetal extracts, highlighting the importance of chiral centers [23, 24]. Similarly, in the recent past our group developed an affinity column with EC to isolate proteins, using a methodology which blocks the C3 hydroxyl group; this approach allowed the isolation of GPER from endothelial cells [25]. However, even when this approach is reliable, it is possible that C3 hydroxyl group blockade could reduce the EC stereoselectivity necessary for its specific interaction with proteins.

With these approaches, we intended to demonstrate that PXR is a possible target for (-)-Epicatechin in skeletal muscle and C2C12 myoblasts.

2. Results

2.1. There are three probable sites for ligands interaction in PXR's LBD

Taking in consideration that homology comparisons between reported pocket of human PXR (hPXR) and mPXR establish a displacement of 3 amino acids residues [26, 27, 28, 29] and the lack of reports of specific amino acids in the binding site (pocket) of the mouse PXR protein, we performed docking assays for 10 ligands that were reported as activators for the mPXR [30] (Table 1). The analysis of 1000 docking assays per molecule, suggested that there are three possible binding sites (Figure 1). Binding site 1 seems to be the most probable of interaction and the one with the highest affinity.

2.1.1. (-)-Epicatechin interacts with PXR ligand binding domain (LBD)

To confirm that PXR specifically, interacts with EC, *in silico* analysis of the affinity characteristics between EC, pregnenolone-16?-carbonitrile (PCN) (a mouse specific agonist) and the ligand binding domain (LBD) of mouse PXR (mPXR) was performed and compare their possible binding sites. The binding site for both molecules seems to be the same (Figure 2A) also most of the interacting atoms of that site are identical as shown in the protein-ligand interactions maps (Figure 2B, C). Furthermore, binding energy of EC is near to that for PCN (Table 1).

2.2. PXR can be isolated from SkM with the EC's affinity column

We developed a chromatography affinity matrix (this approach offers great selectivity, which depends on the ligand's availability/exposure in the matrix) in order to isolate proteins from skeletal muscle. In SkM, EC has demonstrated beneficial effects, mainly an increase in differentiation-inducing molecules and in the maintenance of muscle health [31].

In order to meet our objectives, (-)-Epicatechin was chemically modified using a Mannich type reaction; the modification consisted in the coupling of 6-aminocaproic acid (6-AC) (a “spacer arm”, to increase the relative “freedom” of the attached molecule and by this, decreasing possible steric limitations). A pinkish solid (70% yield) was obtained (compound A). MS (positive ESI mode) m/z: 434.18; (negative ESI mode) m/z: 578.94 (Figure 3). The structures of EC with the modification in the possible reactive sites are shown in Figure 4. (The proportions of the different possibilities formed were estimated theoretically, based on orto-para- director substituents effect on the EC's A ring and based on steric effect). IR spectra also confirm the formation of compound A (Table 2). After the compound A coupling, based on the standard EC's curve, the flavonoid's quantity coupled to the matrix was 90μg (-)-Epicatechin/mL column, giving a 69.32% yield. Figure 5 shows the compound A coupling possibilities to the matrix.

To assess the specificity of the developed column we performed several controls: 1) evaluation of proteins adsorption into the matrix, we evaluated conditions as, number of washes (10 washes with double volume of the column, approximately 3 mL per wash) necessary to eliminate the no interacting proteins into the base matrix, this step was essential to demonstrate that the isolated proteins were not an effect of inner adsorption; essentially, we found no interacting proteins in the control column. 2) evaluation of the possible interaction of proteins with a column treated with all the reactants but no EC, this approach was necessary to demonstrate that even when the EC binding breaks there were no interaction of proteins with a sepharoseB-6ACA column, we found that essentially there were no interaction and 3) evaluation of the most effective method (pH change, ionic strength change and competitive separation) to detach the interacting proteins from the column. The resulting columns allow us to isolate skeletal muscle's PXR (Figure 6B) and some proteins with affinity for EC (not identified, data not shown) (Figure 6A).

2.3. (-)-Epicatechin induced the PXR translocation to the nucleus

To corroborate that EC activates PXR, the translocation of this protein was evaluated through Immunofluorescence. EC induced translocation of PXR to the C2C12 nucleus (Figure 7C), similarly to PCN (Figure 7B); this effect was blocked when cells were stimulated in presence of Ketoconazole (Figure 7D), leading to similar colocalization as C2C12 control group (Figure 7A). Using the Cell Profiler (software) colocalization protocol (Figure 7E) results shown that Ketoconazole was able to block the EC and PCN-induced translocation of PXR, strongly suggesting that EC is a PXR ligand.

2.4. (-)-Epicatechin increases Cyp3a11 expression through PXR activation

We demonstrated the capacity of EC to activate mPXR. The main function of this protein is the elimination of xenobiotics trough the increase of expression of enzymes of Phase I and Phase II of drug biotransformation; one of these enzymes is Cyp3a11 (the mouse analog form of human's Cyp3a4) [29]. Results showed that (-)Epicatechin increase the mRNA expression of Cyp3a11 in C2C12 cultured cells, through the activation of PXR, this effect was blocked by the presence of ketoconazole (Figure 8).

2.5. (-)-Epicatechin induces C2C12 cells differentiation by PXR stimulation

To determine the participation of PXR in some of the effects described previously for EC, we evaluate the capacity of this flavonoid and PCN to induce the C2C12 myoblasts differentiation into myotubes [31, 32]. Results shown that under proliferation conditions (FBS 10%, Control), essentially, there was no differentiation (Figure 9A). Culturing cells with horse serum (2%, positive control) induced differentiation and an increase in Myogenin (a transcriptional activator that promotes transcription of muscle-specific target genes and plays a role in muscle differentiation) expression (Figure 9A, 9B). Remarkably, EC and PCN, under proliferation conditions (FBS 10%) induced differentiation (Figure 9A) and a significant increase in Myogenin (Figure 9B). Both processes were inhibited by the presence of ketoconazole (Figure 9A, 9B).

Interestingly, there was not a full block of EC-induced effects in the presence of the antagonist, leading to the hypothesis of participation of other receptors, like GPER [31].

Table 1. The amino acids reached for ten PXR's activators.

Molecule	Site 1	Site 2	Site 3	Site 4	Energy (Kcal/mol) at Site 1 ± SD[1]
(-)-Epicatechin	Met206, Leu237, Leu240, Ala241, Val243, Ser 244, Met247, Phe248, Phe278, Cys281 Ile282. Phe285, Trp296, Cys298, Tyr303, Leu320, Gln404, Leu408, Ile411, Phe417, Met422, Phe426	His165, Phe166, Lys167, Asp168, Phe169, Arg170, Asp242, Thr245, Tyr246, Lys249, Gly250, Asn253, Thr419	*	*	-8.03 ± 0.08
PCN	Arg203, Met206, Ile280, Leu240, Ala241, Val243, Ser244, Phe248, Phe278, Ile282, Phe285, Trp296, Cys298, Tyr303, Leu320, Gln404, Gln407, Leu408, Ile411, Phe417, Met422, Phe426	*	Phe163, Ser164 His165, Phe166, Lys167, Asp168, Phe169, Leu212, Arg213, Gly214, Glu215, Asp216, Ser218, Ile219, Trp220, Arg300, Leu301	*	-9
Butamifos	Arg203, Met206, Ile208, Leu240, Val243 Ser244, Met247, Phe248, Phe278, Cys281, Ile282, Phe285, Trp296, Cys298, Tyr303, Leu320, Leu408, Met422, Phe426	*	*	Met152, Gln155, Met156, Phe159, Thr161, Arg284, Thr287, Met288, Leu332, His333, Lys334, Tyr337, Val338, Gln341	-7.26 ± 0.06
Mifepristone	*	*	*	Met152, Gln155, Met156, Phe159, Thr161, Thr162, Thr287, Met288, Lys328, Leu332, His333, Lys334, Glu335, Tyr337	/
Prochloraz	Arg203, Met206, Leu237, Leu240, Val243, Ser244, Ala241, Met247, Phe248, Phe278, Cys281, Ile282, Phe285, Trp296, Cys298, Tyr303, Leu320, Gln404, Leu408, Ile411, Phe417, Met422, Phe426	*	*	Met152, Gln155, Met156, Phe159, Thr161, Arg284, Asn286, Thr287, Met288, Lys328, Leu332, His333, Lys334, Tyr337, Val338, Gln341	-7.99 ± 0.20
Phosalone	Arg203, Met206, Leu240, Val243, Ser244, Phe248, Phe278, Ile282, Phe285, Trp296, Tyr303, Leu320, Gln404, Thr405, Gln407, Leu408, Ile411, Phe417, Met422, Phe426	*	*	Gln155, Phe159, Thr161, Thr287, Met288, Lys328, Gln331, Leu332, His333, Lys334, Tyr337	-7.14 ± 0.14
T0901317	Arg203, Met206, Ile208, His239, Leu240, Ala241, Val243, Ser244, Met247, Phe248, Thr277, Phe278, Cys281, Ile282, Phe285, Trp296, Tyr303, Leu320, Gln404, Thr405, Gln407, Leu408, Ile411, Phe417, Met422, Phe426	*	*	*	-9.85 ± 0.32
Flucythrinate	*	*	Thr162, Phe163, Ser164, His165, Phe166, Lys167, Asp168, Phe169, Leu171, Leu212, Arg213, Gly214, Glu215, Trp220, Cys298, Arg300, Leu301	Met152, Gln155, Met156, Phe159, Thr161, Arg284, Thr287, Met288, Lys328, Leu332, His333, Lys334, Glu335, Tyr337, Val338, Gln341	/
Fluvanilate	*	*	Phe163, Ser164, Phe166, Lys167, Asp168, Phe169, Leu171, Leu212, Arg213, Gly214, Glu215, Asp216, Arg300, Leu301	Met152, Asp153, Gln155, Met156, Phe159, Thr161, Leu283, Arg284, Thr287, Met288, Lys328, Gln331, Leu332, His333, Lys334, Tyr337, Val338, Gln341	/
Isofenphos	Arg203, Met206, Ile208, Leu240, Ala241, Ser244, Val243, Met247, Phe248, Phe278, Lys281, Ile282, Phe285, Trp296, Tyr303, Leu320, Gln404, Thr405, Leu408, Ile411, Phe417, Met422, Phe426	*	Phe163, Ser164, Phe166, Lys167, Asp168, Phe169, Leu212, Arg213, Gly214, Glu215, Trp220, Arg300, Leu301	Gln155, Phe159, Thr161, Thr287, Met288, Lys328, Gln331, Leu332, His333, Lys334, Tyr337	-7.13 ± 0.30
Pendimethalin	Met206, Ile208, Leu240. Val243, Ser244, Met247, Phe278, Ile282, Phe285, Trp296, Tyr303, Leu320, Met321, His324, Gln404	*	*	Met152, Gln155, Met156, Phe159, Thr161, Leu283, Arg284, Met288, Thr287, Lys328, Leu332, His333, Lys334, Tyr337, Val338, Gln341	-6.83 ± 06

[1] Energy values are represented in mean ± SD at the lowest energy binding site (Site 1) (n = 1000 docking assays performed). (*) no interaction found.

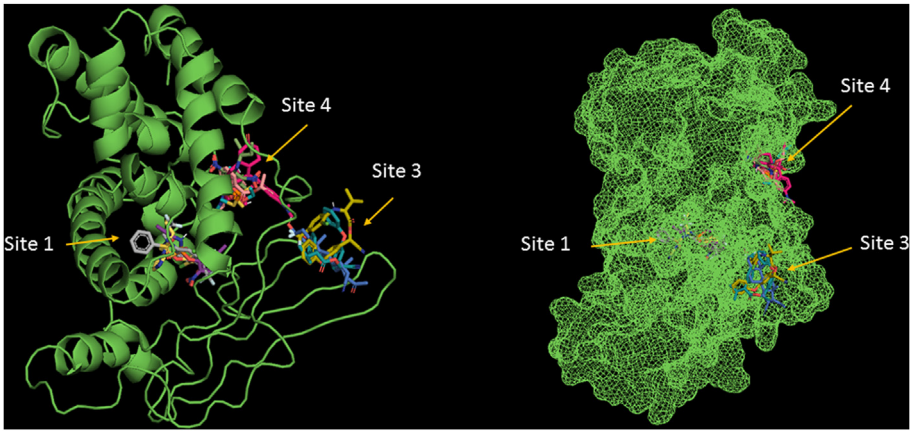

Figure 1. The three most probable binding sites of the 10 mPXR's evaluated activators (ribbons and mesh representation).

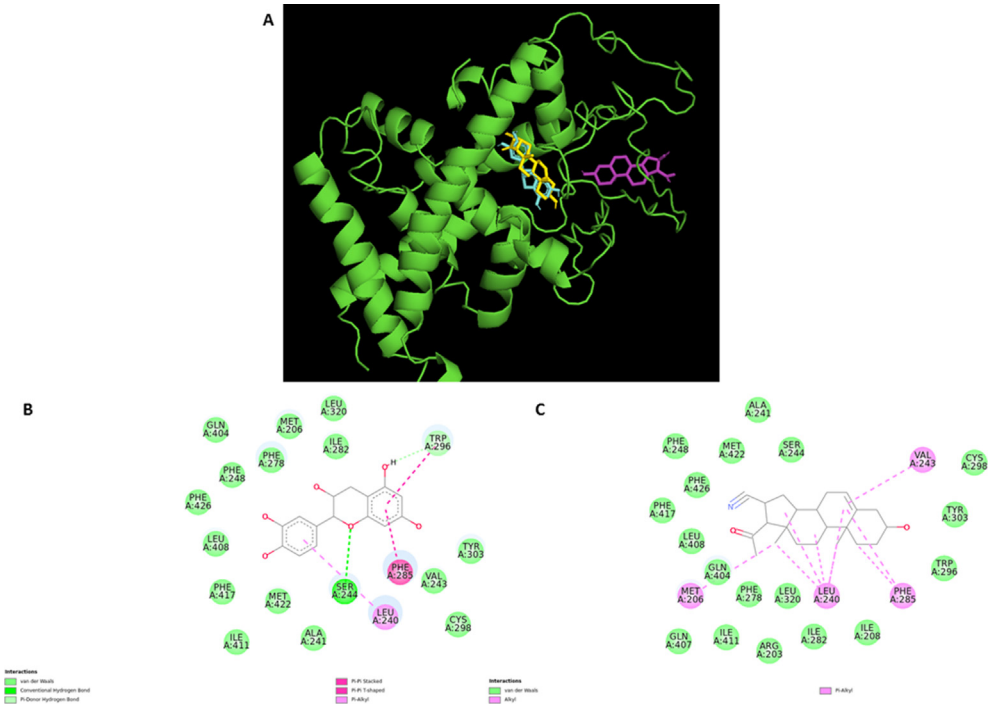

Figure 2. Most probable 3D binding sites for EC (cyan) and PCN (yellow and pink) in mPXR's ligand binding domain (A). Protein-ligand interactions maps with EC (B) and PCN (C).

3. Discussion

The main findings of this work were: 1) (-)-Epicatechin can bind to PXR's LBD, 2) an affinity column of Sepharose 6B-EC was developed using a Mannich type reaction, 3) PXR was isolated from SkM homogenates using the affinity column, 4) (-)-Epicatechin induced the expression of CYP3a11 trough the activation of PXR, 5) EC leads PXR translocation to the nucleus and 6) EC induce C2C12 myoblast differentiation through PXR activation.

Considering, as the main argument, the structural similitude between EC and steroidal backbone, we decided to analyze proteins with receptor characteristics that can recognize this type of structures. We discard estrogen receptors (ERα), since it has been proved that the effects of EC in endothelial cells cannot be blocked with selective antagonist (i.e. tamoxifen) [10] and GPER, whose effects on endothelial cells have already been described [8]. By this and considering the reported effects attributed to the stimuli of this receptor in different tissues [11, 12, 13, 14, 15, 16, 17, 18, 19, 20, 21], the most feasible option was pregnane X receptor (PXR).

To confirm the hypothesis that PXR specifically interacts with EC, in silico analysis of the affinity characteristics between EC, PCN and the LBD of mPXR was performed. Based on the analysis of 1000 docking assays per molecule (included the other eight molecules evaluated), it was suggested that there are three possible binding sites (Figure 2). These results corroborate the idea that de LBD of this protein is promiscuous and that the big area that this domain has could recognize different size and type molecules. It should be noted that these binding sites, were elected based on the most probable position (most repeated) of each compound; nevertheless, position with the lowest energy (~-8.0) seems to be similar to the reported for hPXR (Site 1), just with a little difference in the amino acid type and position. This site includes hydrophobic amino acids mainly: Trp296, Phe285, Tyr303, Leu320 and some amino

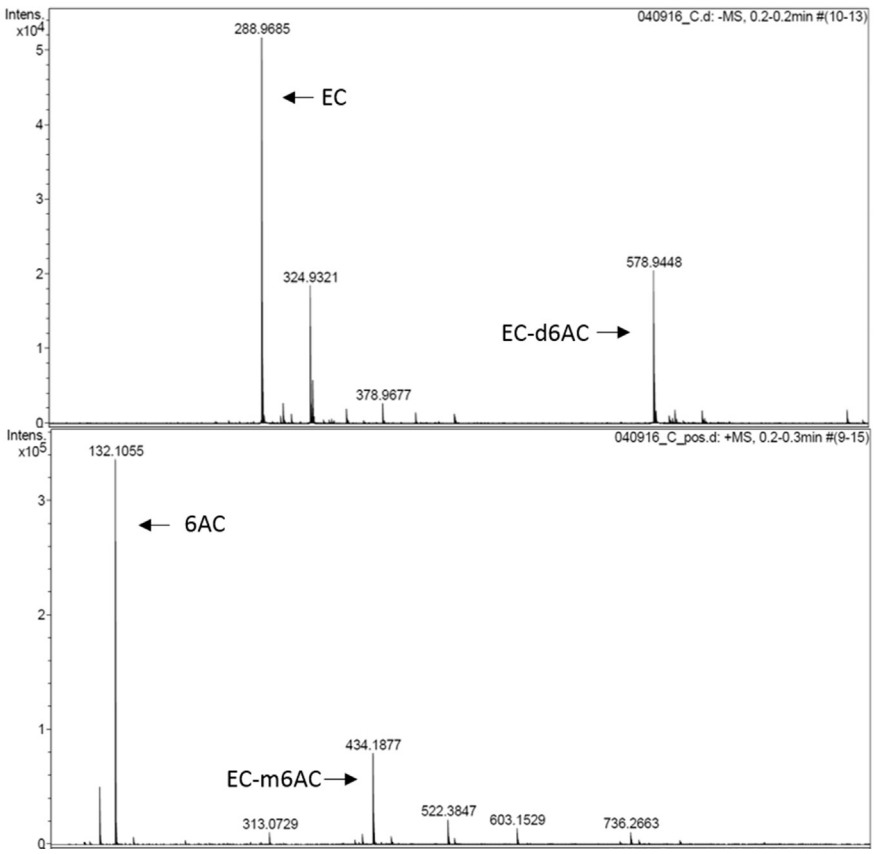

Figure 3. Mass spectra of the obtained compound (Compound A) by the Mannich reaction between (-)-Epicatechin (EC) and 6-aminocaproic acid (6-AC). (A) In negative mode, disubstituted flavonoid (EC-d6AC) m/z: 578.94. (B) In positive mode, monosubstituted flavonoid (EC-m6AC) m/z 434.18.

acids that can form polar contact, (hydrogen bonds), like Ser244, His324 and Gln404 [33]. Some of the evaluated compounds (Figure 1B, 1C and Table 2) contacted the amino acids mentioned above, corroborating that site is occupied for the activation of mPXR. Based in these results we also hypothesize that the different energy values found can lead to differences in the potency that each compound has on mPXR.

In the case of EC, the most favorable binding site was selected (Site 1). At this position, the binding site is characterized by hydrophobic interactions with Trp296, Phe285 and Leu240, these amino acids form an "anchorage" mediated by π-π interactions, maintaining the hydrophobicity of the pocket. In the other hand, Ser244 form an interaction (hydrogen bond) with EC hydrogen at position 3 (ring C) or at position 4 (ring A), this possibility depends on the EC's conformation and on how the groups are disposed in the interacting space; by this analysis, it's probably that the chirality of the ring C could define, at least partially, the stereochemistry effect in mPXR.

We developed a chromatography affinity matrix. In order to meet this objective, (-)-Epicatechin was chemically modified using a Mannich type reaction; the modification consisted in the coupling of 6-aminocaproic acid (6-AC) to the flavonoid through the amino moiety allowing the 6-AC terminal carboxyl group (in basic pH) be attached to the epoxy-activated agarose matrix reaction favored by the chemical activation of the carboxylic group by the addition of carbodiimide. The proposed reaction considered the EC's structural characteristics: no double bond between C2 and C3 carbons, a carbonyl group on C ring, a hydroxyl group in C3 carbon and acidic hydrogens (as is required for Mannich reaction) in the A and B rings. These reasons make this project different compared to another previously synthetized columns [23, 24].

The previously reported reactions differ from our approach since they consider; 1) modifications through the Vilsmeier-Haack and Homer-Wadsworth-Emmons (HWE) reactions, forming a lactone group in the flavanol A ring with the objective to couple the flavonoid to a polyethylene glycol resin with free amino groups [23,24], 2) modifications on EC by the addition of propargyl groups at C3 position in order to couple the flavonoid to an agarose matrix with azide [25].

On the other hand, Mannich reaction even when has not been used for (-)-Epicatechin's aminomethylation, it has been used for flavonoids aminoalkylated analogues formation. On this regard, it has been reported that the amino alkylation substitution can be carried out at A ring's C8 position (as in quercetin [34, 35] and apigenin [36]) and in dihydro flavonols (as in dihydroquercetin [37, 38, 39] and some tannins [40]) in C6 position.

We consider that EC's hydrogens at C6 and C8 positions (Figure 6) are the most susceptible for substitution, due to resonance effect and pH of solution where the reaction takes place, the highest probability is the formation of a disubstituted compound. This is supported by the mass spectra's analysis, where in the negative mode spectra (Figure 3A), the molecular mass peak (m/z) corresponding to the disubstituted compound (6-dAC), likewise the peak corresponding to the monosubstituted compound (6-mAC) in the positive mode spectra (Figure 3B). Inside the mass spectra is possible to see the m/z corresponding to the reagents used for the reaction: (-)-Epicatechin and 6-aminocaproic acid, these signals correspond to the fragmentation's radicals from 6-mAC and 6-dAC, since centrifugation leads compound A separation from no reactive reagents, it did not require purification. Results were supported with data of the IR spectra (Table 3). The positive and negative modes of the mass spectra are complementary in order to determine the binding possibilities of compound A formation, due to if a two molecules of ACA binds to EC forming a "dimer", some of the fragments will appear in the opposite ionization mode, furthermore, flavonoids are susceptible of oxidation in

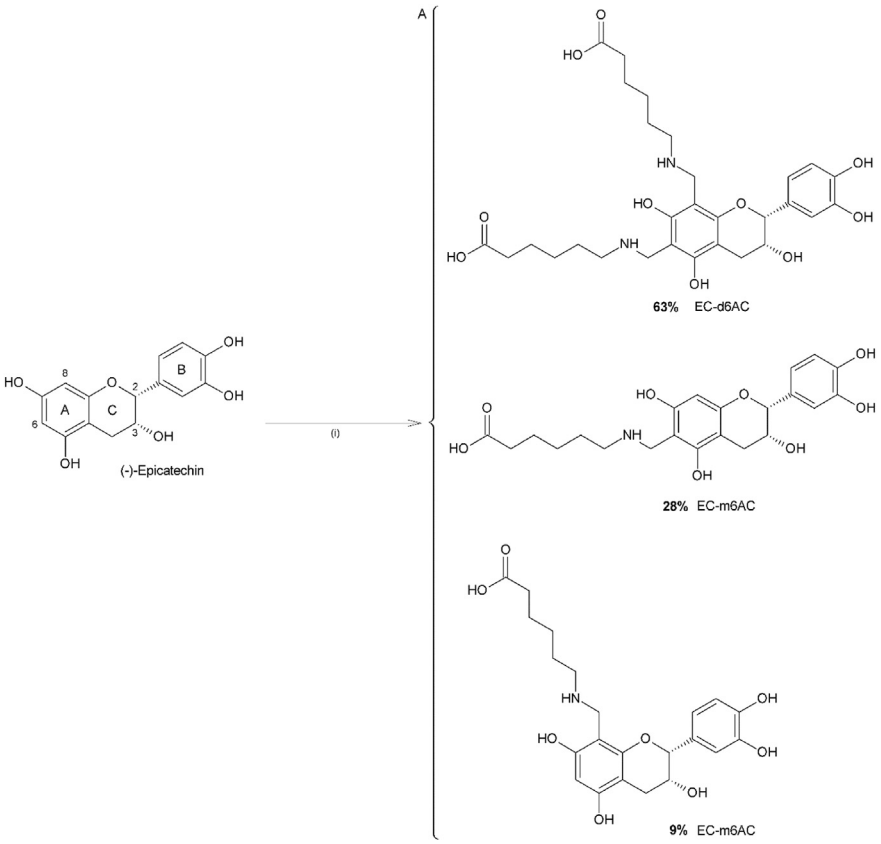

Figure 4. Structure of the possible compounds obtained by the Mannich reaction. (i) Formaldehyde/HCl (conc), 6-AC/NaOH and (-)-Epicatechin/MeOH. 12h, rt. Mono-aminometylated (-)-Epicatechin (EC-m6AC), di-aminometylated (-)-Epicatechin (EC-d6AC).

Table 2. IR bands of the main reagents used in the Mannich reaction and the compound A.

EC		ACA		Compound A	
Functional group	Band (cm^{-1})	Functional group	Band (cm^{-1})	Functional group	Band (cm^{-1})
-OH	3500–3400	-C=O	1450, 1650	-C=O	1469.9, 1621
- Aromatic carbons	1700–1500	- OH	3000–2800	-C-N, -O-H	3392.7
- C-Hsp^3	2900–2980	-$CHsp^3$	2400–2600	-Aromatic carbons	2000–1600
		-N-H	3090	-C-Hsp^3	2989.5

positive mode, so to increase the sensitivity and simplify the spectra, negative ionization was also used.

We also found that the use acidic pH buffers were the best approach, these results agree with reports [41, 42] using similar buffer solutions. The resulting columns allow us to isolate skeletal muscle's PXR (Figure 8B) and some proteins with affinity for EC (not identified, data not shown) (Figure 8A), highlighting that some of them could be specific due to the hydroxyl group in C3 position [25], more work is necessary to identify these proteins.

Finally, we demonstrated the capacity of (-)-Epicatechin to activate mPXR. This conclusion is based in 1) the increase of Cyp3a11 mRNA expression in C2C12 cultured cells, 2) the translocation of this receptor to the nucleus and 3) the induction of C2C12 myoblast differentiation. We believed that, altogether, these results showed that EC is a PXR ligand.

However, the EC-induced effects were not completely annulated in the presence of Ketoconazole, these events raised the possibility of other receptors participating in the phenomena. On this regard, it has been reported that EC can interact with Constitutive androstane receptor (CAR) [43]. We discard this possibility since it was not found in the EC affinity columns protein eluates (data not shown). Other possibilities include GPER (3.)

Results reported here confirm that some of the effects that have been attributed to (-)-Epicatechin are mediated by its interaction with PXR.

It has been proposed that the consumption of products enrich in EC, can improve skeletal muscle quality/performance and also promote myoblast differentiation. In order to reach the concentration of this flavanol that induce the beneficial effects, diverse products can be consumed, mainly those which include cocoa in its content. Pharmacokinetic studies have demonstrated that (-)-epicatechin is highly bioavailable [44, 45], reaching its maximum concentration in plasma after 2h of consumption; as an example, the consumption of a beverage containing 46.7mg of EC, reaches a maximum concentration in plasma of EC of approximately 1 μM, concentration near to the assay in this report [46]. On this way, an inclusion of products with (-)-Epicatechin in the diet, could have positive effects in skeletal muscle.

4. Materials and methods

4.1. Molecular docking

Subsequently to the identification of the possible interaction of pregnane X receptor (PXR) with EC, in silico evaluations were carried out

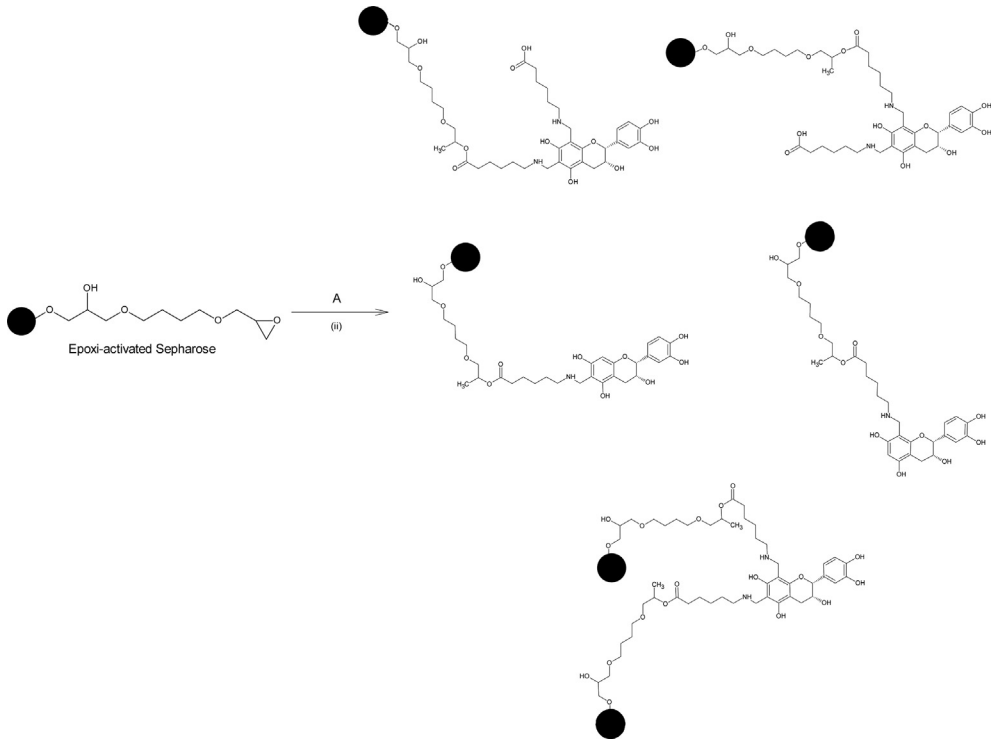

Figure 5. Compound A coupling possibilities to the agarose matrix. (ii) Compound A/MeOH, EDC, carbonate buffer. 12h, rt.

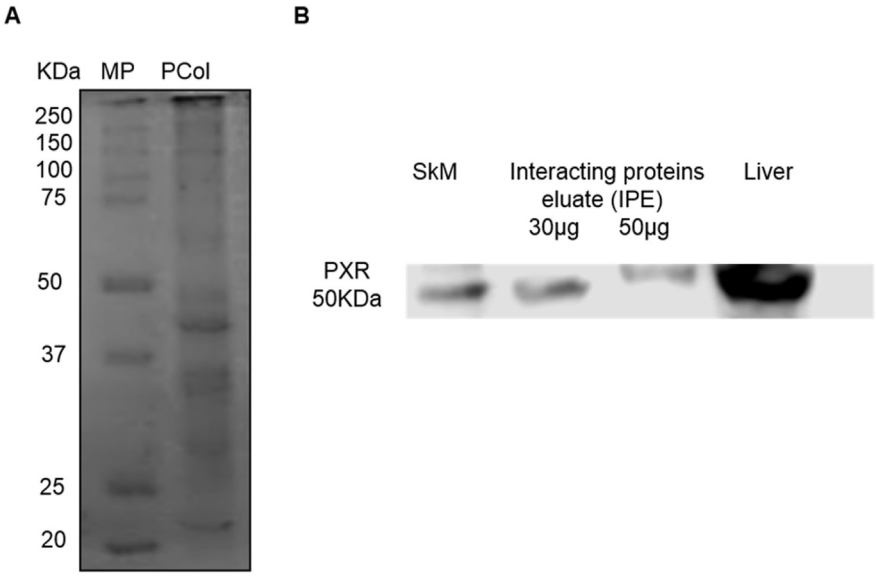

Figure 6. (A) Representative SDS-PAGE electrophoresis separation of the protein mixture showing interaction with the EC-column (staining of proteins was performed with Coomasie blue, image was converted to black/and white for visual facility) (B) representative Western blots identifying PXR in a positive control tissue (liver), in the initial SkM homogenate and in the column interacting proteins eluate (IPE). The complete gel and blot can be seen in supplement material (Columngel and WBPXR).

to identify the most favorable binding site for EC and the compound A (simulating its coupling to the matrix) with PXR. The mouse PXR's Ligand Binding Domain (LBD) protein sequence was downloaded as FASTA format and a 3D sequence was modeled trough the online tool i-Tasser [47]. Model validation (stereochemical quality of protein structure) was performed with PROCHECK software. The energy's structure was minimized to avoid any bad contacts and to evaluate the protein stability with 2ns molecular dynamics using Gromacs parameters [48]. Minimized structure was used to perform 1000 independent blind docking assays in Autodock Vina [49]. The grid center was set on (-3.919, 0.247, 0.522) with a size of 60 × 60 × 60 Å using 1Å of spacing size. The analysis was made using local Unix scripts. Protein-ligand images were made using Pymol and interactions maps were made with Discovery Studio Visualizer. Docking approach was validated with the analysis of PCN interactions.

On the other hand, the 3D (-)-Epicatechin's, PCN and the other 9 evaluated compounds structures were downloaded from PubChem databank (https://pubchem.ncbi.nlm.nih.gov/) and the different possible structures of the compound A were built on MarvinSketch suite (ChemAxon). The structures were refined at ADT: polar hydrogens atoms were added; torsions number was assigned and Gasteiger charges were added.

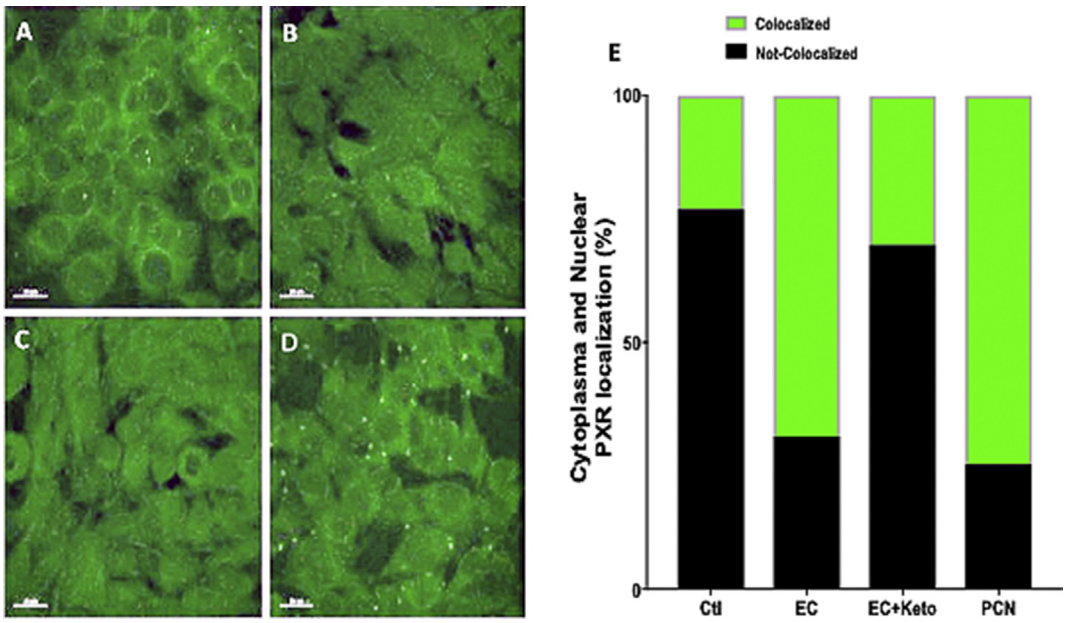

Figure 7. (A) Representative Immunofluorescence images of (A) control C2C12 cells and those stimulated with (B) 0.1μM PCN 20min, (C) 0.1 μM EC 20min and (D) 1 μM Ketoconazole 1h + 0.1 μM EC 20min. (E) Graphic representation of colocalization for the four groups performed by CellProfiler. Images (randomly chose) and Data represent a n = 3 in triplicate.

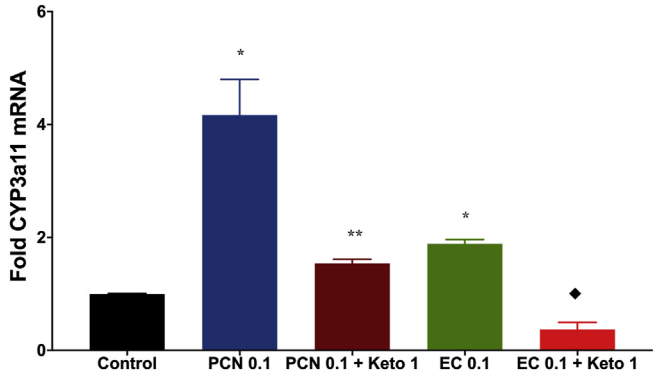

Figure 8. Cyp3a11 mRNA fold expression after the treatment of C2C12 cell culture with EC 0.1μM or PCN 0.1μM in absence and presence of the PXR antagonist Ketoconazole 1μM (n = 3 for each group). Data are presented as mean ± SEM. Kruskal-Wallisś test with Dunn's post-analysis was used to analyze data. Statistical differences were considered when $p < 0.05$ (*vs control) (**vs PCN) (◆vs EC).

4.2. Mannich reaction

A spacer arm was coupled to (-)-Epicatechin using a Mannich type reaction [38]. Briefly: An equimolar (5 mmol) mixture of 37% formaldehyde (Avantor, USA) dissolved in concentrated hydrochloric acid (HCl) (Avantor, USA) and 6-aminocaproic acid (6-AC) (Merck KGaA, Darmstadt, Germany) dissolved in 1N sodium hydroxide (Avantor, USA) was prepared. 5 mmol of EC (Merck KGaA, Darmstadt, Germany) dissolved in methanol were added drop by drop, to the solution; the mixture was stirred at room temperature for about 12 h, under nitrogen atmosphere, until the precipitation of the aminoalkylated EC's derivative (Compound A) was evident (Figure 1). The mixture was centrifugated at 5000 rpm for 10 min, the supernatant was removed, and the sample was dried in vacuum. The compound formation was evaluated trough thin layer chromatography (TLC) and was characterized by infrared spectroscopy (IR) and mass spectrometry (MS). IR methodology: 15mg of vacuum dry compound A was collocated directly on the IR light of the Pike Gladiator equipment, and the reading was performed. OriginPro8 software was used for spectra reading. MS methodology: 15mg of compound A was dissolved in ethanol; the sample was injected directly on the micrOTOF-Q II™ ESI-Qq-TOF equipment, compound A was ionized by electrospray ion source (ESI) in positive and negative modes, using N_2 for nebulization and drying. Data were acquired in MS/MS (auto) scanning mode. Generated ions were analyzed using auto-MSn scan mode. Data acquisition was compared based on LC-NMR/micrOTOF-Q II coupling database.

4.3. (-)-Epicatechin-6-AC coupling to Sepharose 6B

One gram of Sepharose 6B (GE Healthcare Life Science Boston, USA) (washed and treated according supplier instructions) was placed in carbonates buffer (pH = 10.7) and 100 μmol of compound A, dissolved in methanol (Reactivos Química MEYER, México) with 1eq of N-(3-Dimethylaminopropyl)-N'-ethylcarbodiimide (EDC) (Merck KGaA, Darmstadt, Germany) (in order to increase the chemical activation of the 6-AC's carboxylic group of Compound A) were added; the mixture was stirred at room temperature overnight. At the end of the reaction, the mixture was filtered and washed with carbonates buffer (pH = 10.7) to eliminate no reacting compounds; product was washed three times with acetates buffer solution (0.1M, pH = 4.0), Tris-HCl buffer solution (pH = 8.8) and NaCl 0.4 M, to stabilize the column. A control column was prepared without the addition of EC to the matrix.

Additionally, 2 mol of NaBH4 (Avantor, USA) dissolved in Phosphates Buffer Solution (PBS) (pH = 7.4) with 1 mL of concentrated HCl were added to avoid the flavonoid's oxidation. The matrix was dried and stored in PBS (pH = 7.4) at 8 °C. The coupling was evaluated by (-)-Epicatechin's indirect quantification through the vanillin technique for total phenols.

In brief, the vanillin quantification method is based in the reaction of this aldehyde with the flavonoid's structure meta or di substituted rings, generating reddish-pinkish adducts with the most favored orto position. This method was modified according to [50]: Briefly: 100 μL of the sample was mixed with 250μL of a 1% vanillin's methanolic solution and 250 μL of a 25% methanolic sulphuric acid's solution. The mixture was heated at 30 °C for 15 min and the absorbance was measured at 500 nm. A standard curve was built with increasing concentrations (0 a 400 μg/mL) of "free" (-)-Epicatechin.

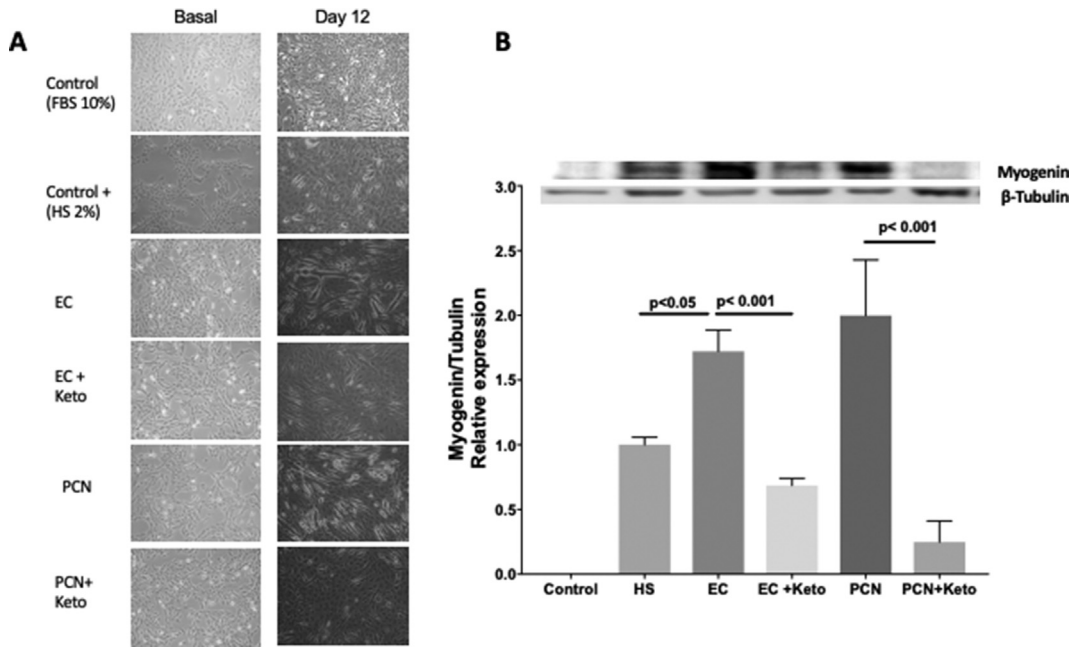

Figure 9. (A) Microscopic representative images of C2C12 differentiation induction without stimulus (Control), with 2% horse serum (positive control) and during treatment EC 1μM or PCN 1μM in absence and presence of ketoconazole 10μM (n = 3 for each group). (B) Myogenin/β-tubulin ratio after the treatment of C2C12 cell culture with EC 1μM or PCN 1μM in absence and presence of ketoconazole 10μM (n = 3 for each group in triplicate). Data are presented as mean ± SEM. ANOVA test (Kruskal-Walliśs with Dunn's post-analysis was used to analyze data). Statistical differences were considered when $p < 0.05$. Data from control was, essentially, no detectable therefore data was normalized against positive control (HS 2%). The complete blot can be seen in supplement material (WBMyogenin) and WBtubulin.

Table 3. Designed primers for the evaluation of Cyp3a11, a downstream gene activated by PXR, and β-actin as constitutive control.

Gene	Reverse Primer (5′-3′)	Forward primer (5′-3′)
Cyp3a11	TGGGTCTGTGACAGCAAGGAGAGGC	ATTCCTGGGCCCAAACCTCTGCCA
β-actin	CCAGTTGGTAACAATGCCATGT	GGCTGTATTCCCCTCCATCG

4.4. PXR isolation and identification

Protocol was reviewed and approved by Institutional Animal Care and Use Committee and carried out in accordance with the NIH Guide for the Care and Use of Laboratory Animals (National Research Council, 2011, https://grants.nih.gov/grants/olaw/guide-for-the-care-and-use-of-laboratory-animals.pdf). Three male Wistar Rats of 230±5g body weight were housed single in polycarbonate cages, with water and food ad libitum, in the Institutional Bioterium under constant humidity and temperature conditions, also ambient dark/light cycles for 1 week. Sterile sawdust was employed as absorbent material covering the whole floor of the cage and was cleaned up three times per week. After this period, rats were euthanized previously anesthetized with a Ketamine (90 mg/kg of body weight) and Xylazine (6 mg/kg of body weight) mixture and a sample of bicep femoris was obtained. The total protein extract was obtained with HEPES 50mM lysis buffer enriched with proteases and phosphatases inhibitors (400 μL/100mg tissue). Protein content was measured by Bradford's method. After that, 200 μg of total protein were incubated overnight at 4 °C and constant stirring for each 0.1mL matrix inside a 5mL plastic chromatography column with a 10 KDa filter. The non-interacting proteins were eluted, and the column was washed several times with PBS (pH = 7.4) until no protein was detected (Bradford's method) in each wash (10 washes were needed) to eliminate adsorbed protein.

Afterwards, 1mL of MES buffer solution (pH = 4.7) was added and the column was incubated overnight at 4 °C to separate the interacting proteins. The affinity column's selective proteins separation was evaluated by SDS-PAGE and a Coomassie Blue stain, comparing both columns eluate and skeletal muscle total protein. For Western Blot assay [51], a 4% stacking gel and a 10% resolving gel were prepared. For each sample 60 μg of protein were loaded and the electrophoresis was carried out at 60V/30 min y 140V/120min. The separated proteins were transferred to a PVDF membrane (Bio-Rad Laboratories, California, USA) under 18V/100min in semi-dry conditions.

The membrane was blocked with 5% free fat dry milk dissolved in Tris Buffer Solution Tween (TBST) (0.1% Tween 20) for 1h. After three washes with TBST, the membrane was incubated overnight with a 1/1000 dilution from the pregnane X receptor (PXR) (ab118336) (Abcam, Cambridge, UK) antibody. A 1/4000 dilution of the secondary anti-mouse (61-6520) (Thermo Fischer Scientific, Massachusetts, USA) antibody, was added after three TBST washes and incubated for 1h. The membrane was developed by chemiluminescence in the LICOR-CDigit equipment (LI-COR Biosciences, Nebraska, USA).

4.5. Evaluation of PXR activation

300,000 C2C12 cells (ATCC® CRL-1772™) were cultured on 50cm2 Petri dishes in DMEM-F12 culture medium supplemented with 10% FBS and 1% antibiotics. Cells were incubated at 37 °C and 5% CO2, until the 90% confluence was reached (approx. 72h). Three groups of cultured cells (2 dishes per group) were formed and they were stimulated with 1) 0.1 μM of EC for 20min, 2) the PXR's agonist (PCN) (Merck KGaA, Darmstadt, Germany) for 20min and 3) the combination of 1 μM of the PXR's antagonist (Ketoconazole) (Merck KGaA, Darmstadt, Germany)

(1h) and 0.1μM of EC (20min). Total RNA was obtained following the procedure of the Direct-zol RNA Miniprep Plus (cat. no. R2051, Zymo Research, CA, USA). cDNA was prepared starting with 1μg of total RNA according to the QuantiTect Reverse Transcription Kit for RT-PCR (Cat No./ID: 20531, Qiagen, USA) instructions. Cyp3a11 (a protein activated after PXR stimulation) mRNA levels were semi-quantitative measured by Real Time PCR with the Biorad's SSofast Eva Green Kit in the StepOnePlus Real-Time PCR System (Thermo Fisher Scientific, Foster City, CA, USA). Primers were designed specifically for the target genes with the Primer designing tool - NCBI – NIH (Table 3). PCR conditions were: 95 °C for 20s, 40 cycles of 95 °C for 15s, 60 °C for 30s. Three independent assay were performed and were co-amplified with β-actin's mRNA as constitutive gen. Results were normalized to the control group by comparative method CT (ΔΔCT).

Also 200,000 C2C12 cells (ATCC® CRL-1772™) were cultured on 8 well glass slides (Lab-Tek II Chamber Slide System 154534) in DMEM-F12 culture medium supplemented with 10% FBS and 1% antibiotics. Cells were incubated at 37 °C and 5% CO2 for 24h, until the 95% confluence was reached. Four groups of cultured cells were formed and were stimulated with 1) No stimulus (Control), 2) 0.1 μM of PXR's agonist (20min) (PCN) (Merck KGaA, Darmstadt, Germany), 3) 0.1μM of EC (20min) and 4) the combination of 1 μM of the PXR's antagonist (Ketoconazole) (1h) (Merck KGaA, Darmstadt, Germany) and 0.1μM of EC (20min). Three independent assays of Immunofluorescence were carried out in order to watch if EC binds and translocate PXR to the nucleus. Cells were fixed to the slide for 7min with cold fresh 4% paraformaldehyde; they were washed twice with PBS-Triton, in order to promote antibody permeabilization. The cells were blocked for 1h with 1:200 Horse Normal Serum (HNS). Cells were incubated for 48 h at 4 °C with 1:750 anti-PXR antibody (ab118336). After that, the anti-mouse FITC antibody (1:1000) was incubated for 24 h at 4 °C. Between each incubation, cells were washed with PBS. Nuclei were stained with Hoechst (0.4%). Fluorescence was observed in the inverted confocal microscope Nikon A1, with blue and green channels. Photographs of three fields for each well were taken at 80x. Furthermore, Cell Profiler [52] colocalization pipeline was used to calculate colocalization of blue and green signals. Images and Data represent a n = 3 in triplicate.

4.6. C2C12 differentiation assay

300,000 C2C12 cells (ATCC® CRL-1772™) were cultured on 50 cm2 Petri dishes in DMEM-F12 culture medium supplemented with 10% FBS and 1% antibiotics. Cells were incubated at 37 °C and 5% CO2, until the 65% confluence was reached (approx. 48h). Six groups of cultured cells were formed and they were cultured with 1) FBS 10% (proliferation conditions, Control), 2) Horse serum (HS, 2%, positive control), 3) 1 μM of EC, 4) 1 μM of PXR's agonist (PCN) (Merck KGaA, Darmstadt, Germany), 5) the combination of 10 μM of the PXR's antagonist (Ketoconazole) (Merck KGaA, Darmstadt, Germany) and 1μM of EC (30min) or 6) 1 μM PCN every 2 days until the 12th day was reached. Every 2 days, photographs were taken. At the end of the assay, total protein was obtained as described above. Protein content was measured by Bradford's method. Myogenin was detected and quantified as a differentiation marker in each group, with Western Blot assay (three independent assays in triplicate), with the same characteristics as those described above, using the anti-myogenin antibody (sc52903).

4.7. Statistical analysis

Prism 7.0 (GraphPad Software, San Diego, CA) was used to perform statistical analyses. Data are presented as mean ± SEM. ANOVA (non-parametric) Kruskal-Walliśs test with Dunn's post-analysis was used to analyze data. Mann-Whitneýs test performed when necessary. Statistical differences were considered when $p < 0.05$.

5. Conclusions

The results reported here demonstrated that (-)-Epicatechin can interact and activate PXR; these results can be the base of further studies to analyze the possible participation of PXR in other skeletal muscle effects shown by EC.

Declarations

Author contribution statement

Miguel Ortiz-Flores: Performed the experiments; Analyzed and interpreted the data; Wrote the paper.

Andrés Portilla-Martínez, Francisco Cabrera-Pérez: Performed the experiments; Analyzed and interpreted the data.

Nayelli Nájera, Francisco Villarreal, Guillermo Ceballos: Conceived and designed the experiments; Analyzed and interpreted the data; Contributed reagents, materials, analysis tools or data; Wrote the paper.

Eduardo Meaney: Conceived and designed the experiments; Analyzed and interpreted the data; Wrote the paper.

Javier Pérez-Durán: Performed the experiments; Analyzed and interpreted the data; Contributed reagents, materials, analysis tools or data; Wrote the paper.

Funding statement

G. Ceballos was supported by Conacyt (253769). F. Villarreal was supported by National Institute of Diabetes and Digestive and Kidney Diseases (DK98717).

Competing interest statement

The authors declare the following conflict of interests: F. Villarreal is a co-founder and stockholder of Epirium Inc. and G. Ceballos is a stockholder.

Additional information

Supplementary content related to this article has been published online at https://doi.org/10.1016/j.heliyon.2020.e05357.

Acknowledgements

Miguel Ortiz acknowledges support from CONACYT in the form of graduate scholarships also to Dr. Vadim Pérez Koldenkova and H.T. Adrián Palma Guzmán from the National Laboratory of Advanced Microscopy, IMSS, where the immunofluorescence assays were performed.

References

[1] J. Shay, et al., Molecular mechanisms and therapeutic effects of (-;)-Epicatechin and other polyphenols in cancer, inflammation, diabetes, and neurodegeneration, Oxid. Med. Cell. Longev. 2015 (2015) 13.

[2] P.R. Taub, et al., Perturbations in skeletal muscle sarcomere structure in patients with heart failure and type 2 diabetes: restorative effects of (-)-epicatechin-rich cocoa, Clin. Sci. (Lond.) 125 (8) (2013) 383–389.

[3] A. Moreno-Ulloa, et al., Recovery of indicators of mitochondrial biogenesis, oxidative stress, and aging with (-)-Epicatechin in senile mice, J. Gerontol. A Biol. Sci. Med. Sci. 70 (11) (2015) 1370–1378.

[4] G. Gutierrez-Salmean, et al., Effects of (-)-epicatechin on molecular modulators of skeletal muscle growth and differentiation, J. Nutr. Biochem. 25 (1) (2014) 91–94.

[5] G. Gutierrez-Salmean, et al., Effects of (-)-epicatechin on a diet-induced rat model of cardiometabolic risk factors, Eur. J. Pharmacol. 728 (2014) 24–30.

[6] M. Zamani, et al., Pre-training Catechin gavage prevents memory impairment induced by intracerebroventricular streptozotocin in rats, Neurosciences (Riyadh) 20 (3) (2015) 225–229.

[7] B. Knezevic, K. Lukowiak, The flavonol epicatechin reverses the suppressive effects of a stressor on long-term memory formation, J. Exp. Biol. 217 (Pt 22) (2014) 4004–4009.

[8] A. Moreno-Ulloa, et al., The effects of (-)-epicatechin on endothelial cells involve the G protein-coupled estrogen receptor (GPER), Pharmacol. Res. 100 (2015) 309–320.
[9] L. Nogueira, et al., (-)-Epicatechin enhances fatigue resistance and oxidative capacity in mouse muscle, J. Physiol. 589 (Pt 18) (2011) 4615–4631.
[10] I. Ramirez-Sanchez, et al., (-)-epicatechin activation of endothelial cell endothelial nitric oxide synthase, nitric oxide, and related signaling pathways, Hypertension 55 (6) (2010) 1398–1405.
[11] J. Hakkola, J. Rysa, J. Hukkanen, Regulation of hepatic energy metabolism by the nuclear receptor PXR, Biochim. Biophys. Acta 1859 (9) (2016) 1072–1082.
[12] V. Lamba, et al., PXR (NR1I2): splice variants in human tissues, including brain, and identification of neurosteroids and nicotine as PXR activators, Toxicol. Appl. Pharmacol. 199 (3) (2004) 251–265.
[13] C. Handschin, U.A. Meyer, Regulatory network of lipid-sensing nuclear receptors: roles for CAR, PXR, LXR, and FXR, Arch. Biochem. Biophys. 433 (2) (2005) 387–396.
[14] E.L. LeCluyse, Pregnane X receptor: molecular basis for species differences in CYP3A induction by xenobiotics, Chem. Biol. Interact. 134 (3) (2001) 283–289.
[15] D.P. Hartley, et al., Activators of the rat pregnane X receptor differentially modulate hepatic and intestinal gene expression, Mol. Pharmacol. 65 (5) (2004) 1159–1171.
[16] Y. Konno, M. Negishi, S. Kodama, The roles of nuclear receptors CAR and PXR in hepatic energy metabolism, Drug Metabol. Pharmacokinet. 23 (1) (2008) 8–13.
[17] A. di Masi, et al., Nuclear receptors CAR and PXR: molecular, functional, and biomedical aspects, Mol. Aspect. Med. 30 (5) (2009) 297–343.
[18] M. Buler, et al., Energy sensing factors PGC-1alpha and SIRT1 modulate PXR expression and function, Biochem. Pharmacol. 82 (12) (2011) 2008–2015.
[19] C.A. Ihunnah, M. Jiang, W. Xie, Nuclear receptor PXR, transcriptional circuits and metabolic relevance, Biochim. Biophys. Acta 1812 (8) (2011) 956–963.
[20] K.E. Swales, et al., Pregnane X receptor regulates drug metabolism and transport in the vasculature and protects from oxidative stress, Cardiovasc. Res. 93 (4) (2012) 674–681.
[21] C. Zhou, Novel functions of PXR in cardiometabolic disease, Biochim. Biophys. Acta 1859 (9) (2016) 1112–1120.
[22] H. Huang, et al., Inhibition of drug metabolism by blocking the activation of nuclear receptors by ketoconazole, Oncogene 26 (2) (2007) 258–268.
[23] C. Chalumeau, et al., Development of an affinity-based proteomic strategy for the elucidation of proanthocyanidin biosynthesis, Chembiochem 12 (8) (2011) 1193–1197.
[24] H. Carrie, et al., New affinity-based probes for capturing flavonoid-binding proteins, Chem. Commun. (Camb) 50 (66) (2014) 9387–9389.
[25] V. Sarmiento, et al., Synthesis of novel (-)-epicatechin derivatives as potential endothelial GPER agonists: evaluation of biological effects, Bioorg. Med. Chem. Lett 28 (4) (2018) 658–663.
[26] S. Ekins, et al., Human pregnane X receptor antagonists and agonists define molecular requirements for different binding sites, Mol. Pharmacol. 72 (3) (2007) 592–603.
[27] M. Banerjee, T. Chen, Differential regulation of CYP3A4 promoter activity by a new class of natural product derivatives binding to pregnane X receptor, Biochem. Pharmacol. 86 (6) (2013) 824–835.
[28] K.D. Mooiman, et al., Milk thistle's active components silybin and isosilybin: novel inhibitors of PXR-mediated CYP3A4 induction, Drug Metab. Dispos. 41 (8) (2013) 1494–1504.
[29] S. Mani, W. Dou, M.R. Redinbo, PXR antagonists and implication in drug metabolism, Drug Metab. Rev. 45 (1) (2013) 60–72.
[30] H. Kojima, et al., Comparative study of human and mouse pregnane X receptor agonistic activity in 200 pesticides using in vitro reporter gene assays, Toxicology 280 (3) (2011) 77–87.
[31] A. Moreno-Ulloa, et al., (-)-Epicatechin stimulates mitochondrial biogenesis and cell growth in C2C12 myotubes via the G-protein coupled estrogen receptor, Eur. J. Pharmacol. 822 (2018) 95–107.
[32] S.J. Lee, et al., Epicatechin elicits MyoD-dependent myoblast differentiation and myogenic conversion of fibroblasts, PloS One 12 (4) (2017), e0175271.
[33] N. Torimoto-Katori, et al., In silico prediction of hPXR activators using structure-based pharmacophore modeling, J. Pharmacol. Sci. 106 (7) (2017) 1752–1759.
[34] S. Zhang, et al., Nitrogen-containing flavonoid analogues as CDK1/cyclin B inhibitors: synthesis, SAR analysis, and biological activity, Bioorg. Med. Chem. 16 (15) (2008) 7128–7133.
[35] T.R. Helgren, et al., The synthesis, antimalarial activity and CoMFA analysis of novel aminoalkylated quercetin analogs, Bioorg. Med. Chem. Lett 25 (2) (2015) 327–332.
[36] R. Liu, et al., Nitrogen-containing apigenin analogs: preparation and biological activity, Molecules 17 (12) (2012) 14748–14764.
[37] N.V. Kosheleva, et al., Synthesis of the first dihydroquercetin–cytisine conjugates, Chem. Nat. Compd. 50 (3) (2014) 443–445.
[38] N.V. Kosheleva, et al., Use of the Mannich reaction to synthesize spin-labeled derivatives of the natural flavonoid dihydroquercetin, Chem. Nat. Compd. 50 (2014) 261–265.
[39] T.S. Kukhareva, V.A. Krasnova, E.E. Nifant'ev, Alkylaminomethylation of dihydroquercetin, Russ. J. Gen. Chem. 75 (2005) 1553–1555.
[40] J. Beltrán-Heredia, J. Sánchez-Martín, M.C. Gómez-Muñoz, New coagulant agents from tannin extracts: preliminary optimisation studies, Chem. Eng. J. 162 (3) (2010) 1019–1025.
[41] J. Zhu, et al., Immobilized fusion protein affinity chromatography combined with HPLC–ESI-Q-TOF-MS/MS for rapid screening of PPARγ ligands from natural products, Talanta 165 (Supplement C) (2017) 508–515.
[42] Z.R. Wang, et al., Identification and purification of resveratrol targeting proteins using immobilized resveratrol affinity chromatography, Biochem. Biophys. Res. Commun. 323 (3) (2004) 743–749.
[43] R. Yao, et al., Dietary flavonoids activate the constitutive androstane receptor (CAR), J. Agric. Food Chem. 58 (4) (2010) 2168–2173.
[44] G. Borges, et al., Absorption, metabolism, distribution and excretion of (-)-epicatechin: a review of recent findings, Mol. Aspect. Med. 61 (2018) 18–30.
[45] A. Moreno-Ulloa, et al., A pilot study on clinical pharmacokinetics and preclinical pharmacodynamics of (+)-epicatechin on cardiometabolic endpoints, Food Funct. 9 (1) (2018) 307–319.
[46] S. Ellinger, et al., Low plasma appearance of (+)-Catechin and (-)-Catechin compared with epicatechin after consumption of beverages prepared from nonalkalized or alkalized cocoa-A randomized, double-blind trial, Nutrients 12 (1) (2020).
[47] Y. Zhang, I-TASSER server for protein 3D structure prediction, BMC Bioinf. 9 (2008) 40.
[48] M.J. Abraham, et al., GROMACS: high performance molecular simulations through multi-level parallelism from laptops to supercomputers, SoftwareX 1–2 (2015) 19–25.
[49] O. Trott, A.J. Olson, AutoDock Vina, Improving the speed and accuracy of docking with a new scoring function, efficient optimization, and multithreading, J. Comput. Chem. 31 (2) (2010) 455–461.
[50] B. Sun, J.M. Ricardo-da-Silva, I. Spranger, Critical factors of vanillin assay for catechins and proanthocyanidins, J. Agric. Food Chem. 46 (10) (1998) 4267–4274.
[51] T. Mahmood, P.C. Yang, Western blot: technique, theory, and trouble shooting, N. Am. J. Med. Sci. 4 (9) (2012) 429–434.
[52] C. McQuin, et al., CellProfiler 3.0: next-generation image processing for biology, PLoS Biol. 16 (7) (2018), e2005970.